Saturation of an optical transition by a phase-diffusing laser field

M. W. Hamilton,* K. Arnett, and S. J. Smith
Joint Institute for Laboratory Astrophysics, University of Colorado and National Bureau of Standards, Boulder, Colorado 80309-0440

D. S. Elliott
School of Electrical Engineering, Purdue University, West Lafayette, Indiana 47907

M. Dziemballa and P. Zoller
Institut für Theoretische Physik, Universität Innsbruck, Technikerstrasse 15, 6020 Innsbruck, Austria
(Received 23 December 1986)

The dependence of the optical Autler-Townes effect on laser field phase fluctuations describable by a two-dimensional Markovian process (phase-diffusion model with a non-Lorentzian line shape) is investigated experimentally in atomic sodium. An intense cw laser tuned to near resonance with the $3S_{1/2}(F=2,M_F=2)\rightarrow 3P_{3/2}(F=3,M_F=3)$ transition was frequency modulated to generate phase fluctuations with the desired characteristics. A weak probe laser coupling to the $4D_{5/2}(F=4, M_F=4)$ state was used to obtain the double-peaked optical Autler-Townes absorption profiles in order to investigate their dependencies on band shape, bandwidth, intensity, and detuning of the intense fluctuating laser field. Reversals of the peak-height asymmetry and reversion to normal asymmetry with increased detuning were observed and measured. Quantitative studies of the spectral widths and splittings of the peaks are also reported. Measured absorption profiles are in excellent agreement with calculations based on previous theoretical work.

I. INTRODUCTION

It is now quite clear that laser field fluctuations play a very important role in nonlinear optical processes. As an example of such sensitivity to fluctuations, we wish to present here the results of an experiment in which we studied the saturation of an atomic transition in the presence of well-characterized laser frequency fluctuations. In this experiment we used the optical Autler-Townes effect to study the ac Stark splitting of the upper level in the saturated transition. Some preliminary results were presented in a recent communication.[1] Here we wish to give a more complete account of the experiment and a comparison to the predictions of a theory[2] that fully takes into account the statistical properties of the laser field.

When one saturates a transition between two states ($|1\rangle$ and $|2\rangle$ in Fig. 1), the strong electromagnetic field causes each level to split into two components. This splitting together with an accompanying shift in the center of gravity of the split components by half the atom-laser detuning is called the ac Stark effect. One may probe the two ac-Stark-split components of one of the states with a weak laser field that couples the probed state to a third ($|3\rangle$ in Fig. 1). The absorption spectrum of this probe field has two peaks, each corresponding to one of the ac-Stark-split components. This is known as the Autler-Townes effect.[3]

A theoretical treatment of the effect of laser fluctuations on the Autler-Townes effect was presented some fifteen years ago in a paper by Zusman and Burshtein.[4] This was motivated by earlier experimental studies[5] of the ac-Stark effect in a strongly driven transition between two excited levels of potassium. In the experiments, the saturation (by a pulsed ruby laser) was probed by measuring the absorption from the ground level to the lower level of the strongly driven transition. Zusman and Burshtein considered different models for the strong laser field, including ones with phase, frequency, or amplitude and phase fluctuations (based upon a jump or random telegraph model) but did not make comparisons with the earlier experiments. Unfortunately, because their S-matrix approach explicitly excluded the possibility that the saturated transition might include the ground level, it was unsuitable for interpreting the results of subsequent experiments.

A number of people published results of experiments[6] in which the strongly driven transition included the

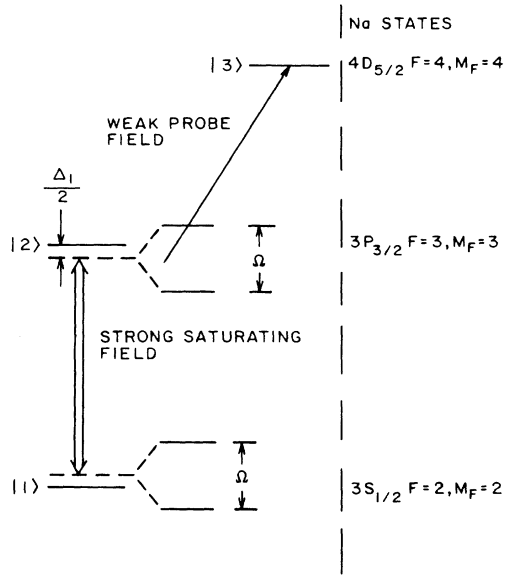

FIG. 1. Atomic level scheme used in these optical Autler-Townes effect experiments. The sodium levels pertinent to our experiment are indicated at the right.

ground level, as in Fig. 1. These works used cw excitation of various transitions, and the expected dependencies of the ac-Stark splitting on laser intensity and detuning were observed. Later experiments[7,8] using broadband pulsed lasers showed features that were in qualitative disagreement with the monochromatic theory.[9] In particular, when the saturating field was detuned somewhat from the transition, the peak-height asymmetry of the Autler-Townes doublet was opposite to that predicted by the monochromatic theory. If, however, the saturating field was detuned far from the transition, the symmetry reverted to its "monochromatic" behavior. This effect was ascribed to the nonmonochromatic character of the pulsed-laser excitation.

The model illustrated in Fig. 2 is particularly useful in giving a qualitative interpretation of this effect where there is a reasonably large atom–saturating-laser detuning, Δ_1, and where collisional effects can be neglected. If $|\Delta_1|$ is greater than both the atomic natural width and the Rabi frequency, one of the absorption peaks occurs at a probe frequency offset $\Delta_2 \simeq -\Delta_1$, i.e., the sum of the saturating laser frequency and probe-laser frequency equals the $|1\rangle \rightarrow |3\rangle$ transition frequency. This corresponds to a direct coherent two-photon excitation of the atom, and is shown schematically as process A in Fig. 2. The other peak in this limit of large $|\Delta_1|$, shown as process B in Fig. 2, corresponds to $\Delta_2 \simeq 0$, i.e., the probe laser is tuned directly to the $|2\rangle \rightarrow |3\rangle$ transition frequency. This peak corresponds to a two-step process whereby the probe laser excites atoms residing in the intermediate $|2\rangle$ state. When the saturating laser is very narrow band, this intense, off-resonant source cannot populate the intermediate state efficiently, and the two-step process is strongly dominated by the two-photon process, a condition which is referred to as normal asymmetry. If, however, the saturating laser is spectrally broad, the intermediate level can become populated directly through the absorption of energy from the wings of the laser spectrum. Thus, it is possible for the two-step process to dominate the two-photon process, so that the peak-height asymmetry is reversed.

This interpretation was substantiated by two experiments, one in which the saturating radiation was produced by a pulsed dye laser whose output could be spectrally narrowed by an extracavity étalon[10] and the other that used stabilized single-mode cw dye lasers.[11] In the former, the asymmetry for large detunings, $|\Delta_1|$, was found to be normal with the étalon in place, but reversed with the étalon out. The latter experiment, with narrow-band lasers, gave results that agreed quantitatively with the monochromatic theory.

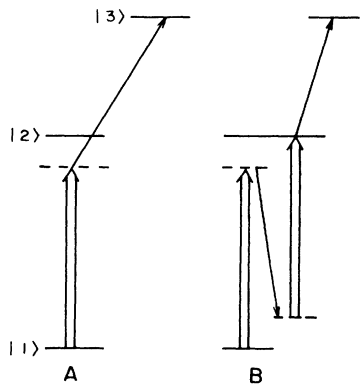

FIG. 2. Two most probable channels for off-resonance excitation to the upper level ($|3\rangle$ of Fig. 1). The broad arrow represents the saturating laser. Process A is called the "two-photon" process and B the "two-step" process.

A theoretical approach which assumes δ-correlated frequency fluctuations[12] produces a reversal of the peak-height asymmetry for all detunings of the saturating laser from the transition frequency, in clear contradiction to the experimental results of Hogan *et al.*[8] Such frequency fluctuations correspond to Lorentzian laser-power spectra and imply an unrealistically large spectral density in the far wings of the laser field. A later theory[2] based on exponentially correlated frequency fluctuations (corresponding to a non-Lorentzian laser line shape) successfully predicted the reversed asymmetry for small saturating laser detunings, and the reversion to normal asymmetry for larger detunings. This latter theory is the one to be reviewed in this paper and is the one to which we shall compare the experimental data.

In all of the previous experiments in which the transition was saturated with a noisy laser the fluctuations were rather poorly characterized. This was an unavoidable consequence of using multimode pulsed lasers in which the fluctuations were a complicated mix of amplitude and frequency fluctuations. The fluctuations are largely environmentally initiated and are thus very difficult to characterize. The experiment to be described below overcame this problem by using a stabilized cw laser to which properly characterized fluctuations were added through extracavity modulation.

In Sec. II we shall review the theory to which our experimental results will be compared. This will then be followed by a section that presents the experimental method. Section IV is a discussion of the results including the comparison with theory.

II. THEORETICAL BACKGROUND

In this section we shall briefly summarize the main features of the theory which will provide the basis for comparison with the experimental data to be presented in Sec. IV. For our theoretical model we assume a laser with constant electric field amplitude E_0, and mean angular frequency ω_0,

$$E = \tfrac{1}{2}(E_0 e^{-i[\omega_0 t + \phi(t)]} + \text{c.c.}) \ . \tag{1}$$

The stochastically varying phase, $\phi(t)$, obeys the Langevin equation

$$\frac{d\phi(t)}{dt} = \omega(t) \ , \tag{2a}$$

$$\frac{d\omega(t)}{dt} = -\beta\omega(t) + F(t) \ . \tag{2b}$$

Here $\omega(t)$ is the stochastic part of the laser frequency and $F(t)$ is a random Gaussian force with correlation function

$$\langle F(t)F(t')\rangle = 2b\beta^2\delta(t-t') \ . \tag{3}$$

Together, the phase $\phi(t)$ and frequency form a two-dimensional Gaussian Markovian process. From the correlation function

$$\langle \omega(t)\omega(t')\rangle = b\beta e^{-\beta|t-t'|} , \tag{4}$$

we are able to identify the parameter $1/\beta$ as the correlation time of the frequency fluctuations. The spectrum of the laser light with phase fluctuations according to Eq. (2) is given by the Fourier transform of the correlation function

$$\langle e^{i\phi(t)-i\phi(t')}\rangle = \exp\left[-b\left[(t-t')+\frac{e^{-\beta(t-t')}-1}{\beta}\right]\right] , \quad t>t' . \tag{5}$$

For $b \ll \beta$ (fast frequency fluctuations) the spectrum tends toward a Lorentzian in shape with full width at half maximum (FWHM) $2b$, but which has wings which begin to fall off faster than a Lorentzian at frequencies $\sim\beta/2\pi$. In the limit of small β (slow frequency fluctuations) the spectrum becomes Gaussian with FWHM $(8b\beta\ln 2)^{1/2}$. Note that in the limit $\beta\to\infty$ the frequency correlation function Eq. (4) becomes δ correlated, so that according to Eq. (2a), $\phi(t)$ would obey a Wiener-Levy process. Strictly speaking, the term "phase diffusion" applies only to the case $\beta\to\infty$. However, we shall use the term to include this generalized phase-diffusing field where β is finite.

In an Autler-Townes-effect experiment one observes the ac-Stark splitting of a strongly driven transition between states $|1\rangle$ and $|2\rangle$ with energies $\hbar\omega_1$ and $\hbar\omega_2$, respectively, using a weak probe laser which induces a transition to another state $|3\rangle$ with energy $\hbar\omega_3$ ($\hbar\omega_3>\hbar\omega_2>\hbar\omega_1$). In particular, one monitors the population of state $|3\rangle$ as a function of the detuning of the probe field by detecting fluorescence from $|3\rangle$. Assuming that the weak, monochromatic probe field with amplitude E' and angular frequency ω' does not affect the strongly driven transition $|1\rangle\to|2\rangle$, the slowly varying density matrix elements obey the system of equations

$$\begin{aligned}
&\left[\frac{d}{dt}+\kappa_3\right]\rho_{33} = i\tfrac{1}{2}\Omega'\rho_{23}+\text{c.c.} ,\\
&\left[\frac{d}{dt}+i\Delta_2+\tfrac{1}{2}\kappa_{23}\right]\rho_{23} = -i\tfrac{1}{2}\Omega'\rho_{22}+i\tfrac{1}{2}\Omega e^{-i\phi}\rho_{13} ,\\
&\left[\frac{d}{dt}+i\Delta_1+i\Delta_2+\tfrac{1}{2}\kappa_{13}\right]\rho_{13} = -i\tfrac{1}{2}\Omega'\rho_{12}+i\tfrac{1}{2}\Omega e^{i\phi}\rho_{23} ,\\
&\left[\frac{d}{dt}+\kappa_2\right]\rho_{22} = i\tfrac{1}{2}\Omega e^{-i\phi}\rho_{12}+\text{c.c.} ,\\
&\left[\frac{d}{dt}+i\Delta_1+\tfrac{1}{2}\kappa_{12}\right]\rho_{12} = i\tfrac{1}{2}\Omega e^{i\phi}(\rho_{22}-\rho_{11}) ,\\
&\rho_{22}+\rho_{11}=1 .
\end{aligned} \tag{6}$$

Here κ_2 and κ_3 are the spontaneous widths of states $|2\rangle$ and $|3\rangle$, respectively; $\Delta_1=\omega_0-\omega_{21}$ and $\Delta_2=\omega'-\omega_{32}$ are detunings, and $\Omega=2\mu_{21}E_0$ and $\Omega'=2\mu_{32}E'$ denote the Rabi frequencies for the $|1\rangle\to|2\rangle$ and $|2\rangle\to|3\rangle$ transitions, respectively, with μ_{21} and μ_{32} being the corresponding dipole matrix elements divided by $\hbar$. In Eq. (6), $\kappa_{ij}=\kappa_i+\kappa_j$ $(i,j=1,2,3)$, defines the off-diagonal decay constants ($\kappa_1=0$).

In the case of monochromatic excitation ($\phi=$const), Eqs. (6) are readily solved for the stationary excited population,

$$\rho_{33} = \frac{1}{4}\frac{(\Omega')^2}{\kappa_3}\left[\frac{1}{2}\frac{\Omega^2}{2\kappa_2|R|^2/(R+R^*)+\Omega^2}\right] \times\frac{T+R^*\kappa_2/(R^*+R)}{ST+\frac{1}{4}\Omega^2}+\text{c.c.} , \tag{7}$$

where

$$\begin{aligned}
R &= \tfrac{1}{2}\kappa_{12}+i\Delta_1 ,\\
S &= \tfrac{1}{2}\kappa_{23}+i\Delta_2 ,\\
T &= \tfrac{1}{2}\kappa_{13}+i\Delta_1+i\Delta_2 .
\end{aligned} \tag{8}$$

For the Rabi frequency Ω much larger than the decay constants κ_{ij}, the population ρ_{22} as a function of Δ_2 shows two peaks which are separated by approximately $(\Delta_1^2+\Omega^2)^{1/2}$. For off-resonance excitation ($\Delta_1\neq 0$) the doublet spectrum is asymmetric as was discussed in Sec. I.

For $|\Delta_1| \gg \Omega,\kappa_2$, Eq. (7) yields the limiting cases discussed in the Introduction, namely, off-resonant two-photon absorption ($\Delta_2\simeq-\Delta_1$) and two-step excitation ($\Delta_2\simeq 0$). For a monochromatic exciting laser the two-photon line is proportional to the intensity of the strong laser, while the two-step line goes with the square of the intensity.[12] Therefore, the two-photon line will be stronger than the two-step line. As remarked earlier, we call this the normal peak asymmetry.

For a stochastic phase, $\phi(t)$, the system of density-matrix equations (6) becomes a system of multiplicative stochastic differential equations. As has been shown in Ref. 2 this set of equations can be solved for the stationary averaged population of state $|3\rangle$,

$$\begin{aligned}
\langle\rho_{33}(t)\rangle &= \frac{i}{2}\Omega'\langle\rho_{23}(t)\rangle/\kappa_3+\text{c.c.}\\
&= \frac{i}{2}\Omega'\left[\frac{i}{2}\Omega\langle\rho_{13}e^{-i\phi}\rangle + \tfrac{1}{4}\Omega'\Omega(\langle\rho_{12}e^{-i\phi}\rangle - \langle\rho_{21}e^{+i\phi}\rangle)\kappa_2\right]\Big/ S\kappa_3+\text{c.c.}
\end{aligned} \tag{9}$$

The averaged density-matrix elements in the second line of Eq. (9) are solutions of the matrix continued-fraction expansion[13]

$$\begin{bmatrix}\langle\rho_{21}e^{i\phi}\rangle\\ \langle\rho_{12}e^{-i\phi}\rangle\\ \langle\rho_{13}e^{i\phi}\rangle\end{bmatrix} = \frac{1}{V_0+\dfrac{1b\beta}{V_1+\dfrac{2b\beta}{V_2+\cdots}}}\begin{bmatrix}\frac{i}{2}\Omega\\ \frac{i}{2}\Omega\\ 0\end{bmatrix} \tag{10}$$

with matrices V_n $(n=01,2,\ldots)$ defined by

$$V_n=\begin{pmatrix} R_n^*+\frac{1}{2}\Omega^2/B_n & -\frac{1}{2}\Omega^2/B_n & 0 \\ \frac{1}{2}\Omega^2/B_n & -(R_n+\frac{1}{2}\Omega^2)/B_n & 0 \\ -i\frac{1}{8}\Omega'\Omega^2/S_nB_n & -\frac{i}{2}\Omega(1-\frac{1}{4}\Omega^2/S_nB_n) & -(T_n+\frac{1}{4}\Omega^2/S_n) \end{pmatrix} \tag{11}$$

and $B_n=\kappa_2+n\beta$, $R_n=R+n\beta$, $S_n=S+n\beta$, and $T_n=T+n\beta$. Equations (9)–(11) are the basis of our quantitative comparison with experimental results in Sec. IV.

The probe absorption spectrum described by Eqs. (9)–(11) for finite-bandwidth excitation shows an enhancement of the two-step process by what we have identified qualitatively as the absorption of photons from the wing of the laser line. This can be sufficient to reverse the asymmetry. For a laser spectrum which falls off faster than a Lorentzian, the absorption from the wings of the spectrum will weaken, thereby reducing the enhancement of the two-step line. Thus, for large detunings, $|\Delta_1|$, and a non-Lorentzian laser line shape, the asymmetry will revert to normal.

To summarize, Eqs. (9)–(11) determine the probe absorption spectrum as a function of the Rabi frequency Ω, the detunings Δ_1 and Δ_2, the spontaneous decay constants κ_2 and κ_3, and the laser bandwidth parameters b and β. Note that the square of the Rabi frequency of the probe, $(\Omega')^2$, factors out from Eq. (9) and thus is part of an undetermined overall scale factor. A refinement that proved necessary was the inclusion of Doppler broadening into the theory. Thus spectra had to be calculated for each velocity group [using Eqs. (9)–(11)] and then averaged over the distribution of velocities.

III. EXPERIMENTAL METHOD

In Fig. 3 we show a schematic diagram of the experiment. Because of its convenient transition wavelengths and natural linewidths, we chose sodium as the atomic species with which to do the experiment. In order to avoid complications due to Doppler broadening and collisions, we used an atomic beam. The randomly modulated transition at 589 nm was used to saturate the $3\,^2S_{1/2}\rightarrow 3\,^2P_{3/2}$ transition, while the probe laser radiation, at 568 nm, weakly coupled the $P_{3/2}$ level to the $4\,^2D_{5/2}$ level (see Fig. 1). The lifetimes of the sodium levels $3P_{3/2}$ and $4D_{5/2}$ are 16 and 50.8 ns, respectively. The probe and saturating beams were combined using an uncoated beam splitter and were collinear in the interaction region. The beam diameters in the interaction region were 0.6 and 0.13 mm for the saturating and probe beams, respectively. The intensity at the center of the saturating beam was varied in the range 0.4–4 W cm^{-2} and the average intensity of the probe beam was ~ 10 mW cm^{-2}. The initial rms frequency fluctuations on the unmodulated saturating laser were ~ 150 kHz and those on the probe laser were ≤ 2 MHz. Both of these numbers are considerably less than $\kappa_2/2\pi$ (10 MHz), which justifies the assumption that these lasers are monochromatic. The saturating laser power was monitored continuously during an experimental run with a thermopile placed behind the laser exit window of the atomic-beam apparatus. Drifts in laser power were compensated for with an attenuator in the rf line to the acousto-optic modulator (AOM) which controlled the fraction of laser power diffracted into the saturating beam. The beams were circularly polarized by a linear polarizer and a Fresnel rhomb placed directly before the window of the atomic-beam apparatus.

The sodium atoms were prepared in the $F=2$, $M_F=2$ ground state using a well-known optical pumping technique.[14] Subsequent excitation with σ^+-polarized light (at 589 and 568 nm) coupled only the $F=3$, $M_F=3$ state of the $3P_{3/2}$ level and the $F=4$, $M_F=4$ state of the $4D_{5/2}$ level. Thus a three-state model for this system is justified.

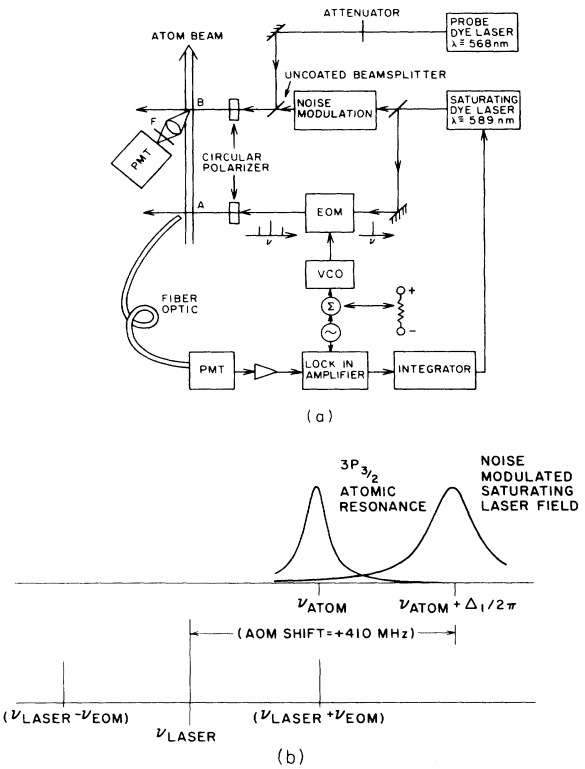

FIG. 3. (a) Schematic diagram of the experiment emphasizing the control loops. A denotes the optical-pumping region and B the saturation region. The frequency of the 589-nm laser is locked by detecting the fluorescence peak at A, and offsetting by the desired detuning Δ_1, minus the 410-MHz offset which is recovered in the AOM noise-modulation process. 330-nm, $4P\rightarrow 3S$ radiation is collected and detected from B as the probe dye laser is scanned over the $3P\rightarrow 4D$ resonance. The interference filter F excludes radiation at laser frequencies. (b) Frequency diagram showing relative positions of the atomic transition frequency ν_{atom}, the saturating field frequency $\nu_{\text{atom}}+\Delta_1/2\pi$, and the optical-pumping-field frequency $\nu_{\text{atom}}=\nu_{\text{laser}}+\nu_{\text{EOM}}$.

The angle at which the saturating beam intersected the atomic beam was adjusted to perpendicularity by minimizing the width of the absorption spectrum of the (heavily attenuated) saturating beam. This adjustment automatically takes into account the deflection of the atomic beam caused by recoil in the optical-pumping region.[11] The Doppler broadening is increased when the laser beam and atomic beam are not perpendicular, because of the broad distribution of atomic velocities in the beam. We measured this $F=2\rightarrow 3$ spectrum by monitoring the fluorescence intensity of the optically pumped sodium at 589 nm, i.e., with the 330-nm bandpass filter (F in Fig. 3) removed, and the probe laser blocked. The minimum width of this single absorption peak was measured to be 12.5 ± 0.5 MHz. This exceeds the 10-MHz natural linewidth of this transition due to the angular divergence of the atomic beam. The above measurement served also as a test of the optical-pumping technique. When the optical pumping beam was blocked, three peaks ($F=2\rightarrow 1$, $F=2\rightarrow 2$, and $F=2\rightarrow 3$) instead of one ($F=2\rightarrow 3$) were seen in the absorption spectrum of the attenuated saturating beam. In order to maintain the orientation of the optically pumped atoms, the distance between the optical-pumping and the saturation regions was kept small (1.5 cm) and a magnetic field of 650 mG aligned parallel to the propagation direction of the laser beams was applied.

The beam used for optically pumping the atomic sodium was derived from the same 589-nm laser source as that which produced the saturating beam. Using an electro-optic phase modulator (EOM), a narrow sideband of approximately 10 mW optical power could be generated, and tuned resonant with the $D2$ transition. The saturating and optical-pumping beams could simultaneously be in resonance because of the $\sim$410-MHz shift in frequency imposed by the noise-modulation system. To observe the Autler-Townes effect, we locked the saturating laser at a fixed detuning and scanned the probe laser through the $3P\rightarrow 4D$ transition. This locking was accomplished by dithering the modulation frequency of the EOM sideband and deriving an error signal from the fluorescence intensity in the optical-pumping region using a lock-in amplifier. This error signal, when fed back to the laser-scan input, locked the saturating field detuning from resonance at a value determined by the difference of the carrier-sideband spacing in the optical-pumping beam and the frequency offset in the noise modulation.

The primary data consisted of absorption spectra produced by scanning the probe laser through the $3P\rightarrow 4D$ transition for each of a series of fixed detunings which were used as the basis of a study of the behavior of the Autler-Townes effect. The absorption spectra were measured by monitoring the 330-nm radiation resulting from decay of the $4D$ level through the $4P$-$3S$ transition, which could be effectively discriminated from scattered laser radiation by use of an interference filter. We chopped the probe beam at 400 Hz and measured the photomultiplier tube (PMT) photocurrent with a high-impedance electrometer and a lock-in amplifier in order to improve the signal-to-noise ratio. The lock-in amplifier output was recorded directly using an X-Y plotter, the abscissa of which was driven by the probe laser scan signal. The intensity of the probe beam was attenuated using neutral density filters to ensure that there were no probe-intensity effects in the probe absorption spectrum. The scan of the probe frequency was calibrated by directing a portion of the probe laser through a spherical mirror Fabry-Perot interferometer of free spectral range 339.1 MHz which produced a subsidiary comb of transverse mode fringes spaced at 25.1 MHz.

We have already described in detail[15] the means by which we produce a laser field with the properties that are described in Sec. II. For the sake of completeness in this paper we will give a brief summary of this technique here. The apparatus for this technique is represented in Fig. 3 by the block labeled "NOISE MODULATION," for which schematic diagrams are shown in Ref. 15. The frequency fluctuations derived from a voltage noise source were applied to the tuning port of a voltage-controlled oscillator. The voltage-controlled oscillator performed a voltage-to-frequency transformation, producing a fluctuating-frequency rf signal with a constant amplitude, which was amplified and used to drive an AOM. In an AOM the laser beam is coherently scattered from an acoustic wave set up by the rf driving field. The net result is a deflection of the laser beam, and the addition of the rf frequency to the optical frequency of the diffracted beam. Thus the mean optical frequency of the diffracted beam was shifted by $\sim$205 MHz, and the frequency fluctuations of the rf signal were transferred to the optical field. In order to cancel the dependence of the diffraction angle on the instantaneous drive frequency, the diffracted beam was redirected through the AOM to be diffracted a second time. Thus the randomly modulated beam had an average frequency that was some 410 MHz greater than that of the unmodulated beam. Use of this double-pass technique had the added advantage of doubling the modulation parameter, thus decreasing the requirements on the driving electronics.

The requirement of a uniform frequency across the laser beam led us to choose a maximum modulation frequency of 6 MHz. In order to augment the frequency-modulation technique, traveling-wave electro-optic modulators (EOM) were used to modulate the laser beam at frequencies in the range of 6 MHz–1 GHz. Phase modulation and frequency modulation are equivalent processes provided the modulating signal is transformed according to the relation

$$P_{\phi}(\omega)=\omega^{-2}P_{\omega}(\omega)\ , \tag{12}$$

where $P_{\phi}(\omega)$ and $P_{\omega}(\omega)$ are the noise-power spectra used for phase and frequency modulation, respectively.

As described previously, the modulation process is completely characterized by the noise spectral density, b, and the correlation time of the fluctuations, β^{-1}. Control of these two parameters was attained through attenuation of the noise-power level, and through the use of active linear shaping networks, respectively. The shape of the noise-power spectrum was controlled to within ± 1 dB of the form determined from Eqs. (4) and (12) over the frequency range 100 kHz–1 GHz.

The noise sources that we used to generate the voltage

fluctuations for this work were based upon the shot noise corresponding to the traversal of electrons across the p-n junction of an avalanche mode noise diode. In the limit of large average currents, this produces fluctuations which follow a Gaussian distribution. We have verified the Gaussian property of the voltage fluctuations by repetitively sampling the noise using a wide-bandwidth waveform digitizer, plotting the distribution function and calculating the moments of the distribution. By confining the voltage-to-frequency conversion to a nearly linear region of the tuning curve of the voltage-controlled oscillator, we ensure that the frequency fluctuations are also Gaussian. This property enables us to characterize the higher-order correlation functions in terms of the lowest-order function $\langle\omega(t)\omega(0)\rangle$, which in turn is specified by the noise-power spectrum. Correlation functions of all orders of the fluctuating frequency are required to specify the laser-power spectrum, which we measure using a heterodyne detector and a rf spectrum analyzer. Thus we are confident that our randomly modulated field is accurately described by the generalized phase-diffusion model.

IV. RESULTS AND DISCUSSION

Before proceeding to discuss the results of the experiment with the randomly modulated laser, we shall present some results where the saturating beam was unmodulated, i.e., monochromatic. This is an important check on the experimental technique. Figure 4 shows a probe absorption spectrum recorded with the monochromatic saturating beam resonant with the $F=2\rightarrow 3$ transition. The experimental data are shown as discrete points. We shall defer discussion of the solid (theoretical) curve until a later paragraph. As mentioned in the Introduction, peak height asymmetry of probe absorption spectra is a sensitive measure of the effect of laser field fluctuations. When the saturating laser is tuned to the atomic resonance ($\Delta_1=0$), the peaks are expected to be equivalent and to be of the same height. As the detuning of the saturating laser is increased, however, the peaks start to differ from each other, with a change in the relative heights (and widths) of the two peaks.

One may define an asymmetry parameter, A, as

$$A=\frac{h_l-h_u}{h_l+h_u}\ , \tag{13}$$

where h_l (h_u) refers to the height of the lower (upper) probe frequency-absorption peak. In Fig. 5 this is shown plotted against the saturating-laser–atom detuning for the case of a monochromatic saturating laser. The experimental data are shown as crosses and a theoretical curve for comparison is shown as a solid line. In the theoretical curve in Fig. 4, there are no free parameters other than the vertical scale. Similarly, there are no free parameters in the theoretical curve in Fig. 5, except for the position of $\Delta_1=0$. These comments will also apply to all of the subsequent comparisons of theory and experiment in this paper. The values of the Rabi frequency and the saturating laser detuning were experimentally determined as described below.

Accurate control and measurement of the saturating laser detuning from resonance was essential to the experiment. To first approximation, this is given by the difference between the carrier-sideband spacing and twice the center frequency of the rf drive to the AOM. However, small errors in the parallelism of the saturating and

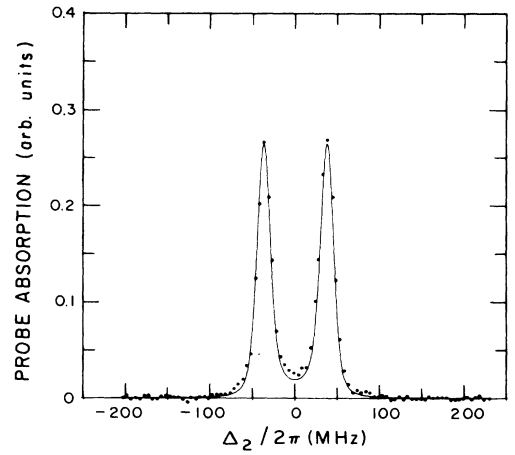

FIG. 4. Probe absorption spectrum taken with a monochromatic saturating field. $\Delta_1/2\pi=0$ MHz, $\Omega/2\pi=75$ MHz. The points represent the experimental data and the solid curve is the theoretical calculation.

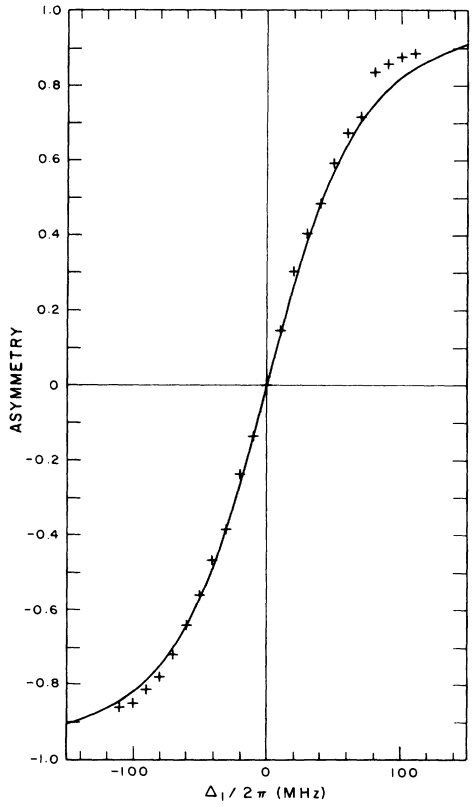

FIG. 5. Asymmetry parameter as a function of Δ_1 for a monochromatic saturating field. $\Omega/2\pi=75$ MHz. Experimental results are represented by + 's. The solid curve is the theoretical calculation.

optical-pumping beams rendered this method unsuitable for precise determination of the point $\Delta_1=0$. Because the experimental geometry remained constant throughout each data set (consisting of spectra for varying saturating laser detuning Δ_1 but with parameters b, β, and Ω constant), this method provided the accurate determination of the relative detuning of the saturating beam from the transition frequency. The zero-detuning point was established by finding the frequency of the *monochromatic* saturating laser which yielded a symmetric Autler-Townes spectrum. The determination of $\Delta_1=0$ from the difference between the rf drive frequencies was consistent to within ± 5 MHz of that measured by this method.

We also needed an accurate determination of the Rabi frequency, Ω. This was determined from observations of the splitting of the Autler-Townes doublet as a function of saturating laser frequency, as shown in Fig. 6. The solid (theoretical) curve in Fig. 6 was calculated numerically, the value of the Rabi frequency, Ω, used being that which gave the best agreement around $\Delta_1=0$. This value of Ω was then used for the theoretical curves shown in Figs. 4 and 5. For a monochromatic saturating field, the splitting goes, to lowest order in κ_1^2/Ω, as[16]

$$\mathcal{S}=(\Omega^2+\Delta_1^2)^{1/2}-O\left[\frac{\kappa_2^2}{\Omega}\right] . \tag{14}$$

The numerical calculations show that the residual Doppler broadening produces another correction of magnitude roughly equal to the last term in Eq. (14). These corrections are included in all of the theoretical curves. We have also included in Fig. 6 results from monochromatic and nonmonochromatic measurements. These illustrate a point made by Georges and Lambropoulos,[17] that saturation by a phase-diffusing field does not change the size of the ac-Stark splitting from that induced by a monochromatic field of the same intensity. Although this prediction was made in the limits of $\Omega \gg \kappa_i$, b, and also $\beta \to \infty$, i.e., a Lorentzian line shape in the high-intensity limit, our observations with a non-Lorentzian laser line shape show no significant difference from the monochromatic situation. This observation should be contrasted with the prediction that a chaotic field (amplitude fluctuations) would decrease the splitting by a factor of up to $\sqrt{2}$ from that induced by a monochromatic field.[17]

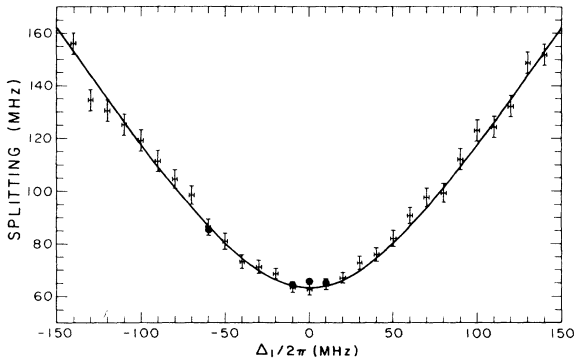

FIG. 6. Observed splittings vs Δ_1; solid circles represent data for monochromatic excitation, + 's for nonmonochromatic excitation. FWHM 14 MHz, $\beta/2\pi=80$ MHz, saturating intensity $=3.7$ W cm^{-2}.

Figure 7 shows the asymmetry parameter as a function of the saturating laser detuning from resonance for different saturating laser spectra and fixed laser intensity ($\Omega=68$ MHz). A sequence of asymmetry curves is shown in which the laser spectrum is nearly Lorentzian in shape [except for Fig. 7(a), which corresponds to the monochromatic case], and the width of the laser increases from very narrow band to 18-MHz full width at half maximum (FWHM). The asymmetry curves can be seen to change continuously from the monotonic form for the narrowband laser to that with a very pronounced reversal of the asymmetry for 18 MHz FWHM. For large-enough detunings the asymmetry always reverts to normal. Recalling Fig. 2 and its discussion (see Sec. I), we can easily explain the progression toward asymmetry reversal in terms of the increasing power in the wings of the saturating laser-power spectrum as one increases the FWHM of the spectrum.

Figure 8 shows another sequence of graphs of A versus Δ_1; this time the parameter that is varied is the saturating intensity (and thus the Rabi frequency). Now we see that increasing the Rabi frequency retards the reversal of the asymmetry. This behavior arises from the fact that on the time scale of the faster Rabi oscillations, the influence of the frequency fluctuations is diminished. Note that Fig. 8(b) has the same data as Fig. 7(c).

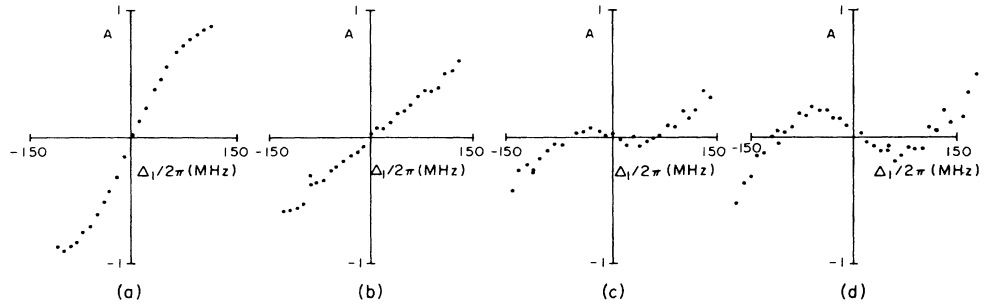

FIG. 7. Sequence of plots of asymmetry parameter vs saturating laser detuning, for $\Omega/2\pi=68$ MHz. The laser FWHM increases from left to right. (a) monochromatic, (b) FWHM 7 MHz, (c) FWHM 13 MHz, (d) FWHM 18 MHz. For (b), (c), and (d), $\beta/2\pi=80$ MHz.

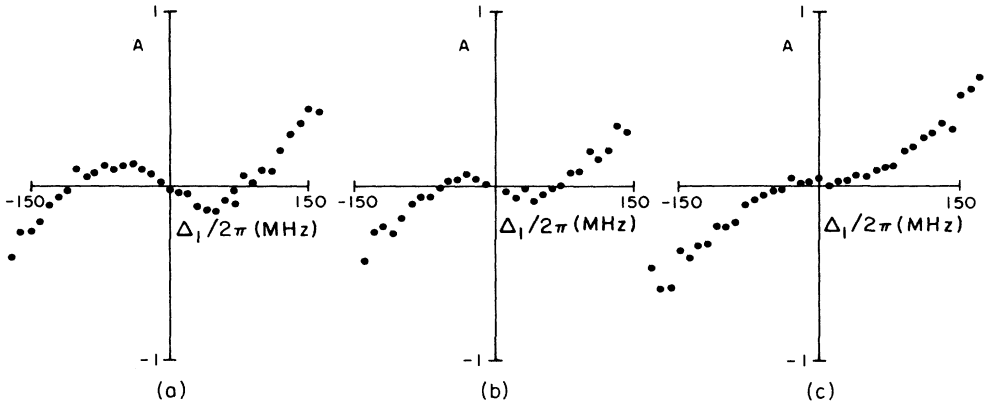

FIG. 8. Sequence of plots of asymmetry parameter vs saturating laser detuning, for increasing Rabi frequency Ω. FWHM 13 MHz, $\beta/2\pi=80$ MHz, and for (a) $\Omega/2\pi=48$ MHz, (b) $\Omega/2\pi=68$ MHz, and (c) $\Omega/2\pi=96$ MHz.

The next sequence of asymmetry curves, Fig. 9, shows their dependence on the shape of the laser spectrum. The solid curves show the theoretical calculations which will be discussed in the next paragraph. In each case the laser width (14 MHz) and the Rabi frequency (68 MHz) are nominally the same. A nearly Gaussian power spectrum results if $\beta/2\pi=10$ MHz as in Fig. 9(a), while for $\beta/2\pi=80$ MHz as in Fig. 9(d), it is nearly Lorentzian. The asymmetry curve for $\beta/2\pi=10$ MHz is indistinguishable from that for the monochromatic data. Qualitatively, this is not unexpected since the wings of a Gaussian-shaped spectrum contain very little power compared to that contained in the wings of a Lorentzian-shaped spectrum. The asymmetry reversal clearly increases as the laser line shape becomes more Lorentzian.

The solid lines in Fig. 9 are the results of calculations based on Eqs. (9)–(11). The calculations are not a fit to the data. The values of the Rabi frequency for those calculations were derived from the splitting at zero detuning. The calculation of the asymmetry curve is insensitive to the precise value of Ω. The values of β and b that were assumed by the theory are simply those that we measured or derived directly from our experimental measurements. These values are shown in Table I. To obtain good agreement, it was important to include the 2.5-MHz residual Doppler broadening in the atomic beam. This was done in the usual way by summing (theoretical) probe absorption spectra over the detunings presented by different velocity classes. Although in Figs. 9(a) and 9(b) we used the measured values of $\beta/2\pi=10$ and 30 MHz, respectively, better fits were obtained for $\beta/2\pi=7$ and 25 MHz, respectively. The discrepancy is probably a result of the ± 1 dB deviation of the actual noise-power spectrum from that prescribed by Eqs. (2) and (12). The scatter in the data points is consistent with statistical uncertainties.

The asymmetry data thus reveal a very pronounced dependence on the laser frequency fluctuations. The important criteria for strong asymmetry reversal seem to be that the laser width be greater than the natural width of the transition, that the correlation frequency of the fluctuations be greater than the Rabi frequency, and that the correlation frequency of the fluctuations also be greater

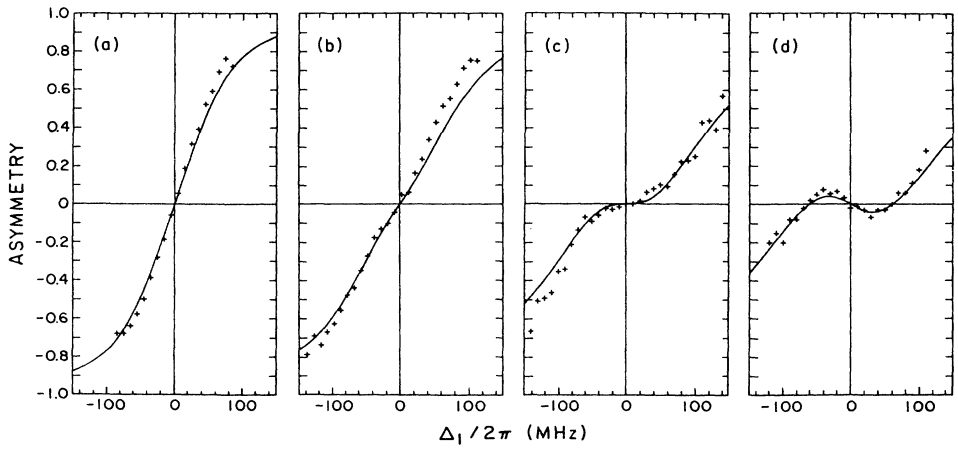

FIG. 9. Sequence of plots of asymmetry parameter vs saturating laser frequency, for increasing values of β. The solid curves indicate the theoretical calculations, parameters of which are tabulated in Table I.

TABLE I. Parameter values for Fig. 9 (all values are in MHz).

Figure part	$\beta/2\pi$	$b/2\pi$	FWHM	$\Omega/2\pi$
(a)	10	8.8	14	67
(b)	30	7.3	14	71
(c)	60	7.1	14	67
(d)	80	7.0	14	64

than the laser linewidth, i.e., the laser-power spectrum is nearly Lorentzian.

The next feature of the probe-absorption spectra that we wish to discuss is the width of the two peaks, specifically in the limit of large $|\Delta_1|$. When the detuning of the saturating laser from resonance is much greater than the Rabi frequency and the natural width of the transition, the two peaks can be identified as corresponding to a two-photon process and a two-step process, as described earlier. The linewidth of each of these peaks should depend upon the following terms:

$$\Delta\nu_{\text{two photon}} \sim \Delta\nu_{\text{sat. laser}} + \frac{\kappa_3}{2\pi} + \Delta\nu_{\text{probe laser}} ,$$

$$\Delta\nu_{\text{two step}} \sim \frac{\kappa_2}{2\pi} + \frac{\kappa_3}{2\pi} + \Delta\nu_{\text{probe laser}} .$$

(Here $\Delta\nu$ represents the spectral FWHM of the quantity indicated by the subscript.) The summation indicated in these relations is, strictly speaking, only valid for the case of weak fields and Lorentzian laser line shapes, but it is useful to consider this approximation in order to highlight some interesting physics.

The width of the two-photon absorption peak is expected to depend linearly upon the width of the saturating laser and should not depend upon the width of the intermediate $3P$ level. This is based upon the role of the $3P$ level in providing a near-resonant enhancement of the two-photon transition rate without actually becoming populated in the process. Our measurements of the FWHM of the two-photon peak as a function of laser linewidth are shown in Fig. 10(a). All data corresponding to nearly Lorentzian laser line shapes (i.e., $\beta/2\pi = 80$, 100 MHz) are included in this diagram. The line of unit slope would be expected to fit the data if all widths could be simply summed. The data points are derived by averaging the widths of the two-photon peaks as measured on about six probe absorption spectra on each side of resonance with the greatest detuning, $|\Delta_1|$, and a reasonable signal-to-noise ratio. Averaging data with positive and negative Δ_1 helps decrease systematic errors introduced by the nonlinearity of the probe laser scan. The uncertainty of the width averages is estimated to be about 2 MHz.

The width of the two-photon peak should also have some dependence upon the shape of the laser spectrum. In the weak-field limit, the absorption peak would be a convolution of the atomic response with the laser line shape, so that a Lorentzian laser line shape would result in a broader peak than a Gaussian line shape. The data in Fig. 10(b) support this argument. Small $\beta/2\pi$ corresponds to a nearly Gaussian laser line shape. The linewidth of the two-photon peak is somewhat smaller than that for the nearly Lorentzian data ($\beta/2\pi = 80$–100 MHz) but the uncertainties in the data are too large to draw any firm conclusion in this case.

The FWHM of the two-step peak, on the other hand,

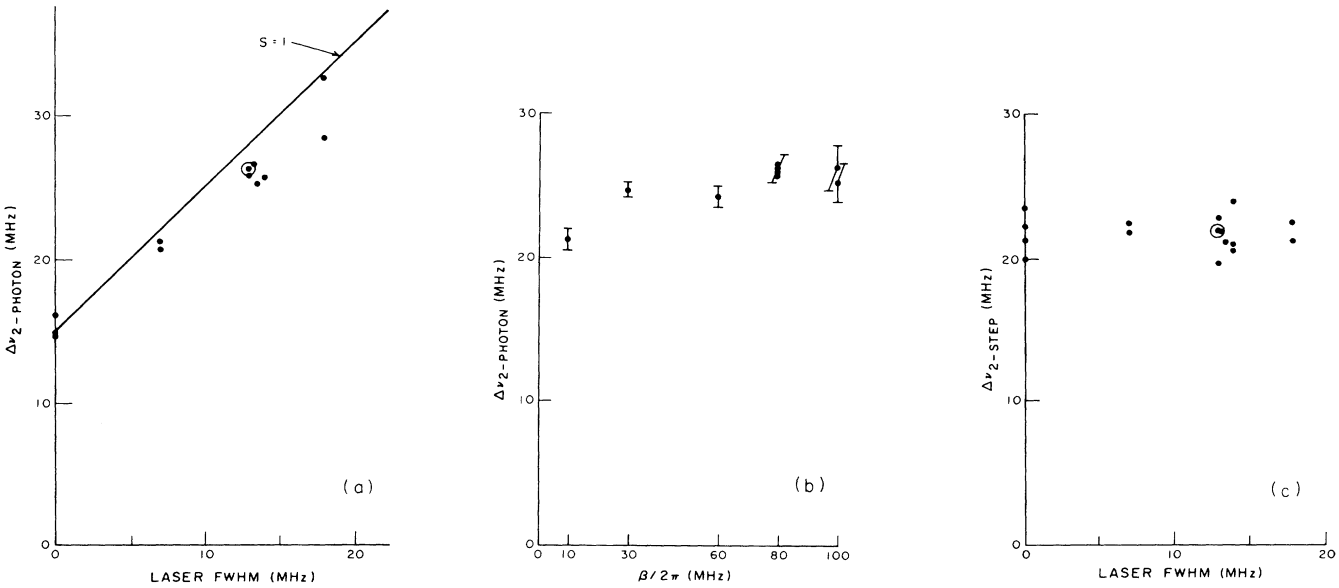

FIG. 10. Dependence of peak widths of Autler-Townes spectra on optical field parameters. These results indicate data for all intensities of the saturating lasers. (a) Width of the two-photon peak as a function of laser bandwidth for Lorentzian power spectra ($\beta/2\pi = 80$–100 MHz). S is the slope of the line. (b) Width of the two-photon peak as a function of $\beta/2\pi$. FWHM 14 MHz. (c) Width of the two-step peak as a function of laser bandwidth, for all values of the frequency correlation parameter β. The circled points in (a) and (c) each represent two superposed points.

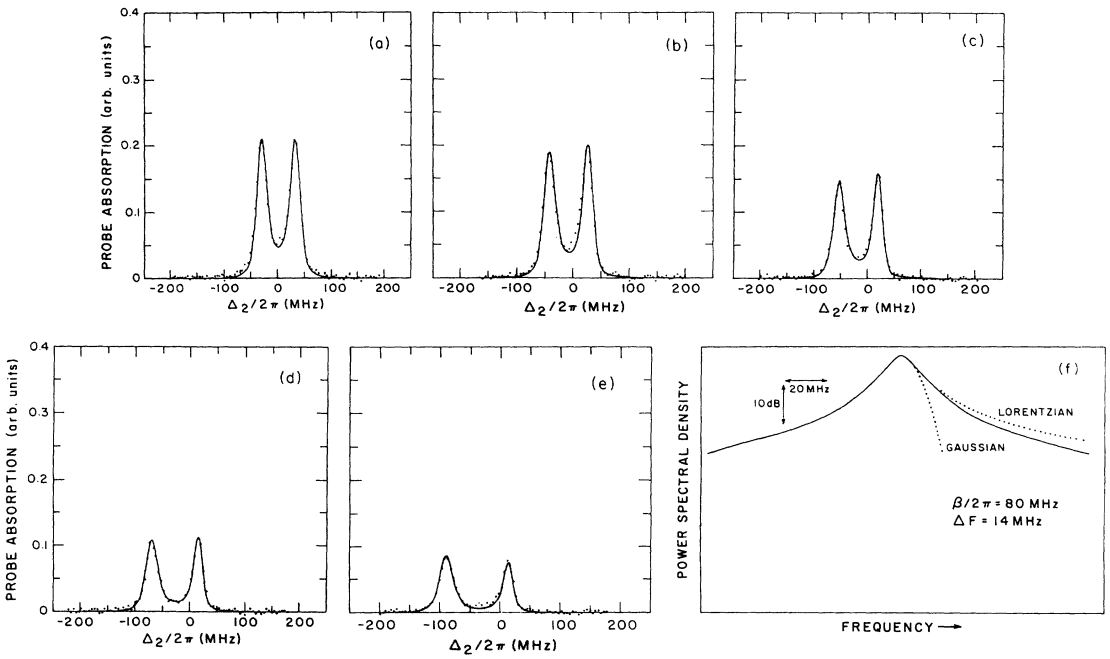

FIG. 11. (a)–(e) Comparison of measured probe absorption spectra with theoretical predictions (solid curves). Laser detunings and Rabi frequencies are listed in Table II. (f) The saturating laser-power spectrum used to obtain the data in (a)–(e). ΔF is the FWHM. Note that the vertical scale is logarithmic. A Lorentzian and a Gaussian line shape of the same FWHM are shown (· · · ·) for comparison.

should not increase with increasing laser width. Since this peak corresponds to excitation from the $3P$ to the $4D$, with little concern for how the $3P$ level was initially populated, the saturating laser width is not important in this process. Figure 10(c) is a plot of the observed width of the two-step peak versus laser width. No dependence can be seen.

Finally, we wish to compare the probe absorption spectra directly with the theory of Dixit, Zoller, and Lambropoulos.[2] Shown in Figs. 11(a)–11(e) are probe-laser-absorption spectra taken with a fluctuating saturating field. These were taken with noise characteristics of the saturating laser $\beta/2\pi=80$ MHz and b such that the FWHM of the laser spectrum was 14 MHz. From numerical calculations of the laser spectrum we infer that $b=7.05$ MHz. The data begin with approximately zero detuning and progress in steps of 20 MHz detuning (Δ_1) toward the high-frequency side of the $3S$-$3P$ transition ($\Delta_1>0$). Again the solid curves depict the theoretical predictions with the parameters as listed in Table II. In these plots the experimental data have been digitized only in order to clarify the presentation. The free parameters in this comparison are the vertical scale and the position of the zero in the horizontal axis. The Rabi frequency for each theoretical curve was obtained in the manner described in the discussion of Fig. 6 [thus obtaining Ω (expt) in Table II], although it was also adjusted within the error limits of the measured peak splitting to give the best agreement [see Ω (theor) in Table II]. The noise parameters, β and b, that are used in the theoretical curve are simply those measured experimentally (see Table II).

The value of Δ_1 used in the theoretical curves was obtained by defining $A=0$ to be at $\Delta_1=0$, as discussed earlier. This value is shown as Δ_1 (theor) in Table II. For comparison, Table II also includes Δ_1 (expt), calculated by subtracting the modulation frequency on the optical-pumping beam from twice the AOM drive frequency. Apart from a systematic discrepancy in the fit between the peaks where the data are higher than predicted, the agreement is excellent. We believe that this discrepancy is due to the small variation in saturating field amplitude across the probe beam. This departure from the ideal was not incorporated into the theory. It was necessary, however, to incorporate the residual Doppler broadening of 2.5 MHz into the theory in order to obtain good agreement. If the Doppler broadening was omitted or if it was included by simply increasing the value of the natural linewidths, the agreement between these calculated data and the experimental results was significantly decreased. Figure 11(f) shows the laser-power spectrum used in ob-

TABLE II. Parameter values for Fig. 11 (all values are in MHz).

Figure part	$\Delta_1/2\pi$ (theor)	$\Delta_1/2\pi$ (expt)	$\Omega/2\pi$ (expt)	$\Omega/2\pi$ (theor)
(a)	2	0	64	63
(b)	−18	−20	64	66.5
(c)	−38	−40	64	63
(d)	−58	−60	64	64
(e)	−78	−80	64	70

taining the data of Figs. 11(a)–11(e).

In conclusion, we have demonstrated that fluctuations play an important role in nonlinear optical processes, typified in this case by the saturation of a transition. For the frequency fluctuations that we used, it has proven possible to accurately model the experiment with a theory which takes into account their finite correlation time as well as other nonideal features. Theories which use other models for the fluctuations (chaotic field and random telegraph models) exist now and work is currently under way to test these experimentally.

ACKNOWLEDGMENTS

The experimental research was supported by the U.S. Department of Energy, Office of Basic Energy Sciences. M.W.H. wishes to acknowledge the support of the Science and Engineering Research Council at various stages in the preparation of this manuscript. M.D. and P.Z. acknowledge support from the Jubiläumsfonds der Österreichischen Nationalbank under project number 2604. D.S.E. acknowledges support from the National Science Foundation.

---

*Present address: Department of Physics and Applied Physics, University of Strathclyde, 107 Rottenrow, Glasgow G4 0NG Scotland.

[1]M. W. Hamilton, D. S. Elliott, K. Arnett, and S. J. Smith, Phys. Rev. A **33**, 778 (1986).

[2]S. N. Dixit, P. Zoller, and P. Lambropoulos, Phys. Rev. A **21**, 1289 (1980).

[3]S. H. Autler and C. H. Townes, Phys. Rev. **100**, 703 (1955).

[4]L. D. Zusman and A. I. Burshtein, Zh. Eksp. Teor. Fiz. **61**, 976 (1971) [Sov. Phys.—JETP **34**, 520 (1972)].

[5]A. M. Bonch-Bruevich, N. N. Kostin, and V. A. Khodovoi, Pis'ma Zh. Eksp. Teor. Fiz. **33**, 425 (1966) [JETP Lett. **3**, 279 (1966)].

[6]A. Schabert, R. Keil, and P. Toschek, Appl. Phys. **6**, 181 (1975); Ph. Cahuzac and R. Vetter, Phys. Rev. A **14**, 270 (1976); C. Delsart and J-C. Keller, J. Phys. B **9**, 2769 (1976); J. L. Picqué and J. Pinard, *ibid.* **9**, L77 (1976); H. R. Gray and C. R. Stroud, Jr., Opt. Commun. **25**, 359 (1978).

[7]S. E. Moody and M. Lambropoulos, Phys. Rev. A **15**, 1497 (1977).

[8]P. B. Hogan, S. J. Smith, A. T. Georges, and P. Lambropoulos, Phys. Rev. Lett. **41**, 229 (1978).

[9]See, for example, P. L. Knight and P. W. Milonni, Phys. Rep. **66**, 21 (1980).

[10]D. E. Nitz, A. V. Smith, M. D. Levenson, and S. J. Smith, Phys. Rev. A **24**, 288 (1981).

[11]P. R. Hemmer, B. W. Peuse, F. Y. Wu, J. E. Thomas, and S. Ezekiel, Opt. Lett. **6**, 531 (1981).

[12]A. T. Georges and P. Lambropoulos, Phys. Rev. A **18**, 587 (1978); P. Zoller, J. Phys. B **11**, 805 (1978).

[13]For a discussion of convergence problems, see H. Denk and M. Riederle, J. Approx. Theory **35**, 355 (1981).

[14]J. A. Abate, Opt. Commun. **10**, 269 (1974).

[15]D. S. Elliott, M. W. Hamilton, K. Arnett, and S. J. Smith, Phys. Rev. A **32**, 887 (1985).

[16]L. Allen and J. Eberly, *Optical Resonance and Two Level Atoms* (Wiley, New York, 1975).

[17]A. T. Georges and P. Lambropoulos, Phys. Rev. A **20**, 991 (1979).